

Molecular Dynamics Simulations of Poly(dialkylsiloxanes). Conformational Statistics and Unperturbed Chain Dimensions

Neal Neuburger, Ivet Bahar, and Wayne L. Mattice*

*Institute of Polymer Science, University of Akron, Akron, Ohio 44325-3909, and
Department of Chemical Engineering and Polymer Research Center, Bogazici University,
Bebek 80815, Istanbul, Turkey*

Received October 1, 1991; Revised Manuscript Received December 10, 1991

ABSTRACT: Molecular dynamics trajectories have been computed for isolated poly(dialkylsiloxane) chains in which the alkyl groups are methyl, ethyl, propyl, butyl, isopropyl, isobutyl, or *tert*-butyl. The joint probability profiles for the pair of Si-O bonds flanking a silicon atom are insensitive to the changes in the alkyl substituents. In contrast, the joint probability profiles for the pair of bonds flanking an oxygen atom change systematically as the size of the alkyl group increases. There is a strong correlation in the dihedral angles at these two bonds when the alkyl groups are large. The features in these probability profiles are incorporated into a rotational isomeric state analysis that permits predictions of the characteristic ratio, C_∞ , in the limit as $n \rightarrow \infty$. If the alkyl groups are not branched, the values of C_∞ increase with the size of the alkyl group and reach a limit of about 8.3. Branching of the side chain reduces the characteristic ratio.

1. Introduction

Silicon-containing polymers have applications which include high-performance fluids, elastomers, coatings, surface modifiers, separation membranes, photoresists, soft contact lenses, body implants, and controlled-release systems.¹ An important class of silicon-containing polymers is the poly(dialkylsiloxanes) (PDAS), in which the repeating unit is $-\text{OSiR}_2-$, with $\text{R} \equiv \text{C}_m\text{H}_{2m+1}$. Poly(dimethylsiloxane) (PDMS) is remarkable for its high dynamic flexibility leading to the very low glass transition temperature of about 146 K. It has other unusual properties such as a low characteristic pressure, a low bulk viscosity η , a low-temperature coefficient of η , a low entropy of dilution, and an unusually high permeability.¹ It remains noncrystalline to very low temperatures ($T_m = 313$ K) and may be used at high temperatures due to its excellent thermal stability.^{1,2} Poly(diethylsiloxane) (PDES) and poly(di-*n*-propylsiloxane) (PDPS) have been produced in laboratory scales but do not yet have a commercial application. These polymers have larger alkyl groups than PDMS, which leads to a lower chain flexibility and a higher T_m . PDES and PDPS are reported to exhibit liquid crystalline transitions from the crystalline to the isotropic state via mesomorphic phases.¹ Although the molecular origin of the unusual properties of PDAS is not precisely known, some of them may be attributed to the general structural characteristics of siloxanes such as the relatively long Si-O bonds (1.64 Å), the unusually large angle ($\sim 150^\circ$) for Si-O-Si, and the small size of the O atoms devoid of side groups in the main chain, which produce unusually soft torsional and bending potentials for the Si-O bonds.

In the present work, we investigate the equilibrium statistics and conformational dynamics of a series of PDAS chains by using molecular dynamics (MD) simulations. In recent studies,³⁻⁹ MD trajectories of sufficient duration to sample all conformational space are shown to yield information on (i) the types of isomeric states accessible to backbone bonds, (ii) their probability distribution, and (iii) the mechanism and rate of transitions between them. The formulation of the statistical weight matrices of the *rotational isomeric state* (RIS) formalism¹⁰ via quantitative analysis of MD trajectories has been recently outlined for chains of bonds with symmetric 3-fold rotational potentials.³ The advantages of the application of the approach to polymers with symmetrically disposed

articulated side chains have been mentioned therein. A classical approach, considering the usual first- and second-order interactions alone for the assessment of the probability distribution of isomeric states, becomes inapplicable to those chains in which the interactions between successive bulky side groups and the main chain dominate the behavior of the chain.

MD simulations are performed for methoxy-terminated fragments of PDAS, of the general formula $\text{CH}_3\text{O}[\text{SiR}_2\text{O}]_x\text{CH}_3$, where x is the number of repeat units. Both linear (ethyl, propyl, and butyl) and nonlinear (isopropyl, isobutyl, and *tert*-butyl) side chains have been treated. MD results are analyzed in comparison to those recently obtained for poly(dimethylsiloxane) (PDMS)^{5,6} to elucidate the specific effect of the increasing size of the side groups on the conformational statistics and dynamics of siloxane chains. The results from MD simulations and their implications insofar as the equilibrium statistics of this family of chains is concerned are presented in the current work. In a future paper,¹¹ we will focus on the conformational dynamics of PDAS chains, with particular attention to the extreme member of the family, poly(di-*tert*-butylsiloxane) (PDtBS). Results will be analyzed therein within the framework of the *dynamic rotational isomeric state* formalism.¹²

The organization of the present paper is as follows: The method and results from MD simulations are presented in the next section, together with the qualitative interpretation of the observed probability distribution of conformations on the basis of the specific interactions precluding or favoring specific states. MD simulations indicate that a realistic description of PDAS chains, in terms of the RIS formalism, necessitates the consideration of at least nine equally spaced torsional angles per backbone atom. Accordingly, the conformational space accessible to a repeat unit consists of 9×9 regions whose probabilistic occurrence will be quantitatively analyzed. The statistical weights and energy interaction parameters for various regions of the conformational space, for each member of the family, are presented in section IIIa. Section IIIb will illustrate the use of the information gathered from MD simulations in evaluating the mean-square end-to-end separation of PDAS chains and predicting the influence of the increasing length of the side groups on the unperturbed dimensions of the polymer.

Table I
Number (*N*) of Atoms in the Fragments and Duration of the MD Trajectories

chain	side group	<i>x</i>	<i>N</i>	Δt , ns
PDMS	CH ₃	10	119	2.10
PDES	CH ₂ CH ₃	10	179	0.84
PDPS	[CH ₂] ₂ CH ₃	10	239	0.49
PDBS	[CH ₂] ₃ CH ₃	10	299	0.34
PDiPS	CH[CH ₃] ₂	5	124	0.40, 1.60 ^a
PDiBS	CH ₂ CH[CH ₃]CH ₃	5	154	0.30, 1.10 ^a
PDtBS	C[CH ₃] ₃	5	154	0.60, 1.16 ^a

^a Two independent runs with the indicated durations and different original conformations.

II. MD Simulations. Methodology and Results

The molecular dynamics trajectories were calculated by using SYBYL version 5.3 of Tripos Associates.¹³ Intramolecular degrees of freedom such as bond angle bending, bond stretching, and torsional motion were additively considered with the interatomic van der Waals interactions to evaluate the potential energies of short fragments of PDAS chains. Energy functions supplied by the SYBYL force field were combined with the energy and geometry parameters of Frierson.¹⁴ The same parameters were used in the recent study of PDMS chains, using CHARMM¹⁵ from Polygen Corp.¹⁶ Those parameters were listed in Table I of ref 5. Comparison with previous work demonstrates that, for a given compound, the conformational distribution in space and time is independent of the choice of the software, provided that the same energy and geometry parameters are used as input in both cases.

MD simulations were computed for methoxy-terminated fragments of PDAS chains of *x* = 5–10 monomer units, in vacuum, at 400 K. The type and size of the fragments used in the simulations, their abbreviations, and the duration of the trajectories are listed in Table I. The simulations are long enough to allow for sufficient sampling of conformational space. In all cases, the initial conformation, where all the internal backbone bonds are in the trans state, was minimized by using a conjugate gradient method. The simulation was then performed by using the Verlet algorithm to integrate the equation of motion for all atoms, with time increments of 0.5 fs. Hydrogen atoms were included explicitly. Isothermal conditions were maintained by rescaling the instantaneous velocities of the atoms at intervals of 1 ps.

Examination of the MD trajectories for PDAS reveals that the torsional motion of the main-chain bonds and the bending of the pair of bonds centered about the O atom are the softest modes. That the bond angle for Si–O–Si, θ_b , enjoys a high degree of flexibility was also pointed out in previous studies.^{17,18} It is significantly larger than the almost tetrahedral bond angle θ_a at the Si atom and undergoes occasional inversions inasmuch as the value of 180° is not improbable.

In the case of chains with bulky side groups such as PDtBS, the value of a given bond angle, θ_a or θ_b , is affected by its location along the fragment studied. Internal bond angles are found to be larger compared to the bond angles near the ends of the chain. Inasmuch as the opening of the bond angles helps to relieve the congestion between bulky side groups, this increase in the bending angles as one proceeds toward inner bonds should be expected. A comparative study of the results for different PDAS chains also indicates that both θ_a and θ_b increase with the size of the side groups attached to the siloxane backbone.

The probability distributions depicted in Figure 1a–c illustrate these results. Parts a and b of Figure 1 are obtained for a methoxy-terminated PDtBS fragment of *x*

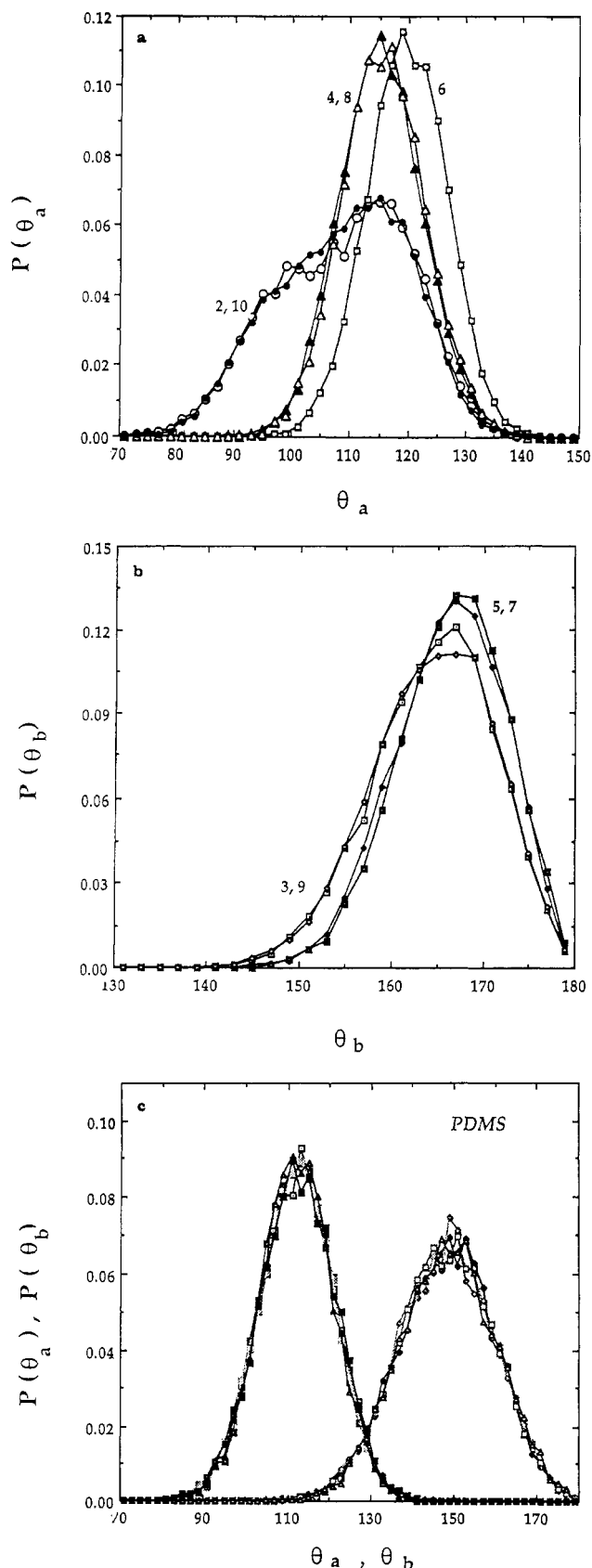


Figure 1. Probability distribution bond angles θ_a and θ_b at (a) Si and (b) O atoms, respectively, in poly(di-*tert*-butylsiloxane), from MD simulations at 400 K. Labels indicate the serial number of Si or O atoms along the methoxy-terminated fragment of 11 backbone atoms. Angles are expressed in degrees. (c) Probability distribution of bond angles θ_a and θ_b in poly(dimethylsiloxane), from MD simulations at 450 K.

= 5 repeat units, for the two successive bond angles θ_a and θ_b . Probability distributions for the bond angles corre-

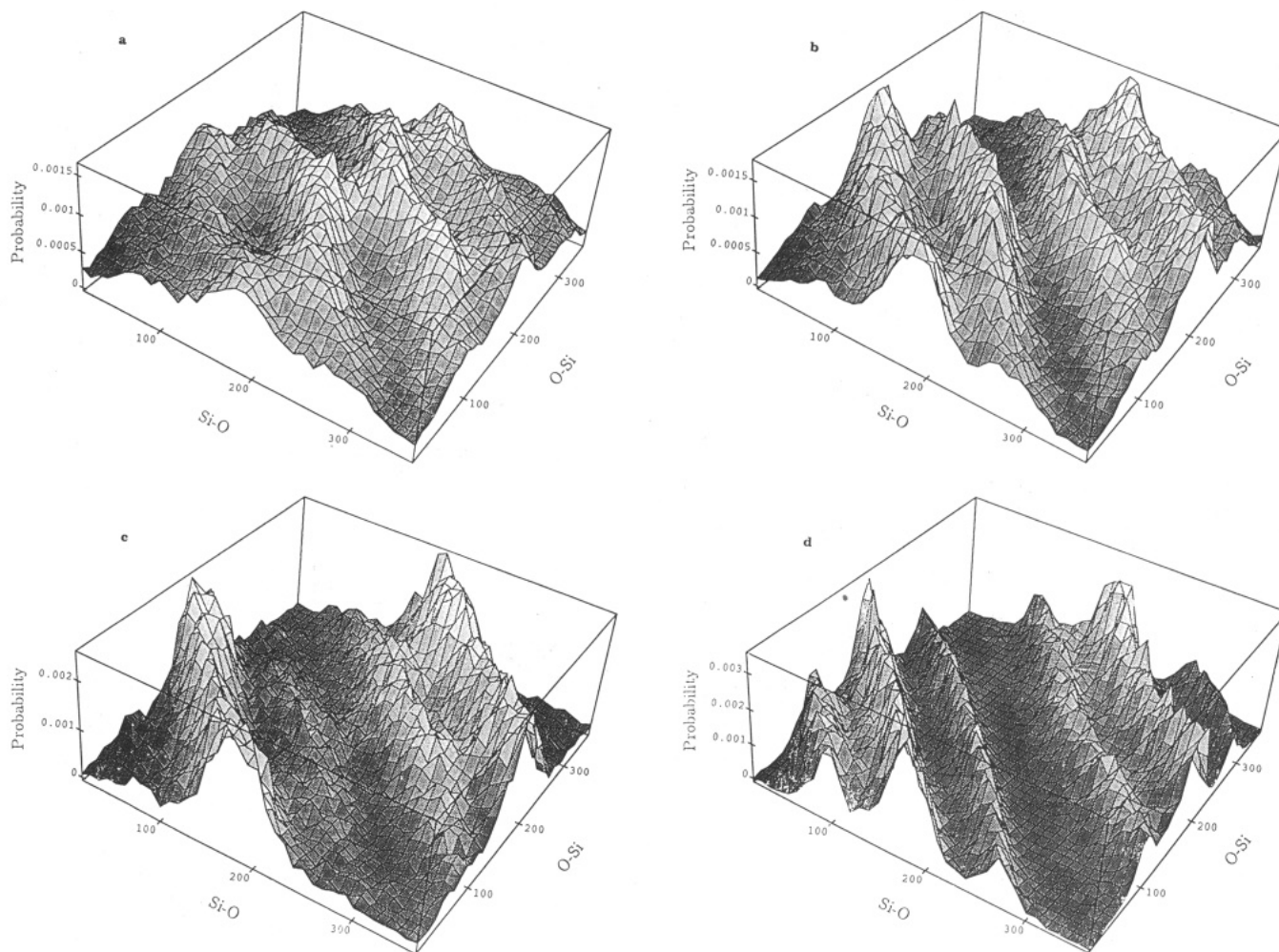


Figure 2. Probability distribution surfaces $P(\phi_i, \phi_{i+1})$ for the torsional angles (ϕ_i, ϕ_{i+1}) of the pair of bonds centered about the O atom in (a) PDMS, (b) PDES, (c) PDPS, and (d) PDtBS, obtained from MD simulations at 400 K.

sponding to different positions along the fragment are labeled by the serial indices of the related internal backbone atoms. Bond angles at Si are found to be more sensitive to the location along the chain, while those at O are less affected. However, no dependence of bond angles on the position along the chain is discernible for PDMS chains, as may be observed in Figure 1c from the superposition of the distribution curves obtained for differential serial number atoms. Comparison of parts a and b of Figure 1 with the equivalent distribution curves obtained for the PDMS fragment of the same size in Figure 1c indicates the broadening of both angles in PDtBS compared to PDMS. Having established the influence of the size of the side group on the value and distribution of bending angles, we now direct our attention to the probability distribution of dihedral angles, which is a major factor distinguishing the different members of the class of PDAS chains.

From the history of dihedral angles, we observe that a wide variety of torsional states are visited by the backbone bonds of all fragments, with substantial fluctuations taking place over time ranges of picoseconds. A closer examination of the time and space distribution of dihedral angles indicates, however, that the torsional motions of the two bonds centered about the oxygen atom are not independent of each other but occur in a concerted fashion. The correlation between adjacent rotations becomes increasingly pronounced with fragments bearing larger side groups. A systematic analysis of pair correlations between neighboring bonds is made possible by the examination

of the probability distribution surfaces constructed as a function of two consecutive bond rotations. Such 3D plots were previously drawn for polyethylene, PDMS, polyisobutylene, and poly(vinyl chloride).^{5,8,9} The basic procedure is to consider the conformational space defined by the complete revolutions of two adjacent bond angles, ϕ_i and ϕ_{i+1} , to divide it into small subspaces, say 36^2 of them, of dimensions $(\Delta\phi_i, \Delta\phi_{i+1}) = (10^\circ, 10^\circ)$, and to record the overall residence time in each subspace. Normalization of the latter yields the probability $P(\phi_i, \phi_{i+1})$ of occurrence of the joint state (ϕ_i, ϕ_{i+1}) representative of a given subspace.

Some probability distributions computed by using this procedure are shown in Figures 2a-d and 3. The panels in Figure 2 are obtained for the pair of bonds centered about the O atom, with the respective fragments of PDMS, PDES, PDPS, and PDtBS. Figure 3 is the probability surface obtained for the pair of bonds centered about the Si atom in PDES. Analogous pictures for the bonds about the Si atom in the other PDAS chains are not presented here, as the basic features remain unchanged. They all show a diffuse distribution of torsional angles showing mild peaks about the rotational isomeric states t , g^+ , and g^- , located at displacements of 0° , $+120^\circ$, and -120° with respect to the t state, and the weak preference, if any, for the tg^\pm or $g^\pm t$ states. The probability surfaces in Figure 2, on the other hand, are of considerable interest. The surface for PDMS in Figure 2a is in good agreement with the one computed using a different algorithm.⁵ The striking feature in those figures is the replacement of peaks

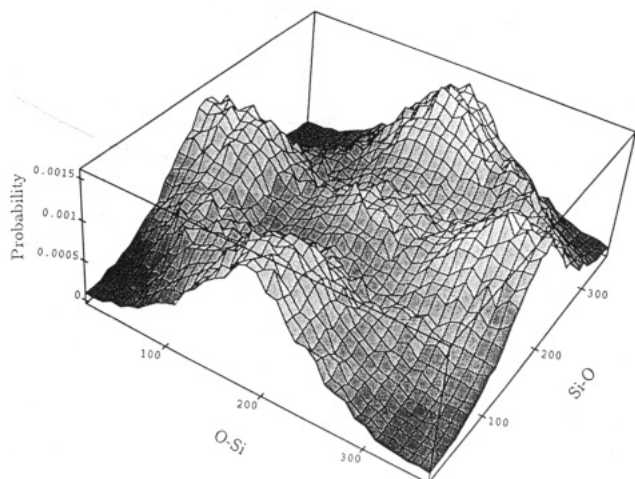


Figure 3. Probability distribution surface $P(\phi_{i-1}, \phi_i)$ for the torsional angles (ϕ_{i-1}, ϕ_i) of the pair of bonds centered about the Si atom in PDES, obtained from MD simulations at 400 K.

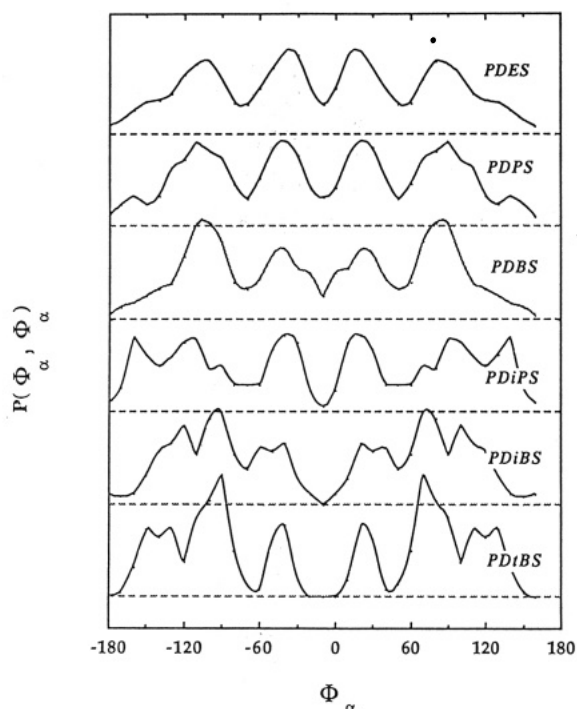


Figure 4. Probability distribution curves along the line $\phi_i = \phi_{i+1}$ of the normalized probability distribution surfaces $P(\phi_i, \phi_{i+1})$ for six fragments. Curves are vertically shifted for clarity. Dashed lines indicate the zero levels for each of the curves. The same scale of range 0.0015 is used for all of the curves.

in PDMS by ridges and valleys, which gradually sharpen with the increasing bulkiness of the side group. Figure 2d obtained for PDtBS is remarkable by its regular structure of ridges.

The gradual evolution of ridges and valleys as one proceeds from PDMS to PDtBS may be followed by examination of the normalized probability curve along the 45° diagonal (the line $\phi_i = \phi_{i+1}$) of the surfaces in Figure 2, as viewed from the top. The family of curves drawn in Figure 4 are obtained by this procedure and allow a comparative study of the distinct behavior of six fragments. The curves are vertically shifted for clarity. The same scale of range 0.0015 has been used for all of them, with the dashed lines representing the zero level for successive curves. In view of the symmetry and periodicity of the conformational space span by two adjacent bond rotations, the ridges observed in PDtBS may be classified

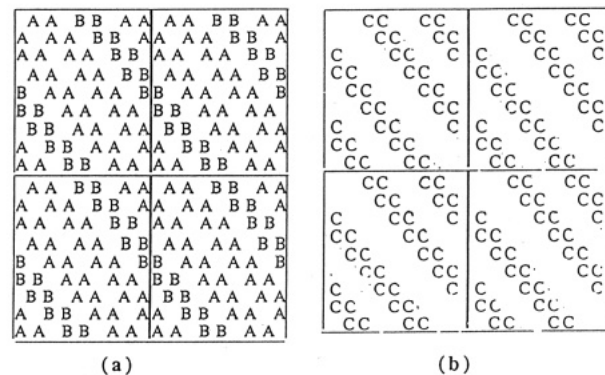


Figure 5. Schematic representation of the types of high-probability ridges observed in the probability surfaces $P(\phi_i, \phi_{i+1})$ for (a) PDtBS and (b) *n*-alkyl-disubstituted fragments with $m \geq 2$. Each dihedral angle covers a range of 720° .

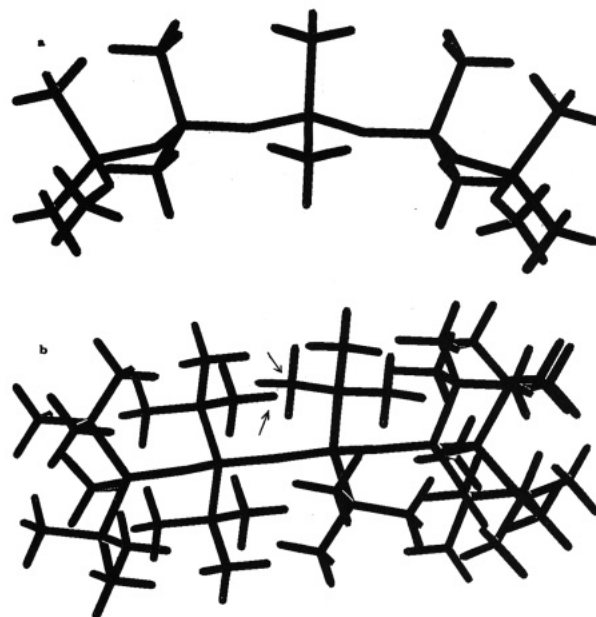


Figure 6. Schematic representation of the planar trans form of (a) PDMS and (b) PDtBS. The molecules are viewed from a position slightly below the plane of the Si and O atoms.

into two distinct types, A and B, while those in PDES, PDPS, and PDBS are all of the same type C, as schematically shown in parts a and b of Figure 5. Two complete revolutions of both dihedral angles are shown in the figures, in order to simplify the visualization of the periodicity in space. A closer examination of the curves in Figure 4 shows that all members of the family exhibit peaks of about the same height at approximately $\Phi_\alpha = \pm 40^\circ$. On the other hand, the next peak located at about $\Phi_\alpha = \pm 80^\circ$ in PDES is gradually split into two peaks, as one proceeds toward members of the family which are subject to stronger steric and energetic interferences near the backbone.

For a better understanding of the specific type and strength of intramolecular interactions leading to the unique probability surface shown in Figure 2d, a closer examination of the spatial distribution of atoms in particular configurations of PDtBS has been carried out and compared with their counterparts in PDMS. Figure 6a shows a methoxy-terminated fragment of a PDMS chain consisting of four monomeric units, all bonds being in the trans planar conformation. The sequence of trans placements is an energetically favorable state. The equivalent configuration assumed by PDtBS is shown in Figure 6b. The methyl groups in PDtBS are rotated about the C-CH₃ bond in order to minimize their steric interferences.

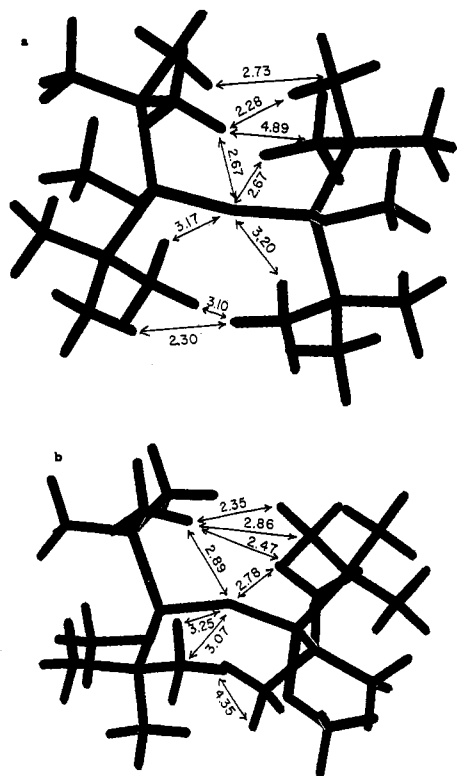


Figure 7. Schematic representation of two energetically favorable conformations along high-probability ridges (a) A and (b) B in PDTBS.

Nevertheless, the methyl groups connected to neighboring units are too close to each other, as is clearly seen in the figure. The separations between nearest nonbonded hydrogen atoms or pairs of C and H atoms belonging to different methyl groups are found to be below 1 Å, which leads to an excessively large repulsive energy. An example is the pair of atoms indicated by the arrows in the figure, the separation of which is 0.82 Å. The overlapping of the van der Waals volumes of the *tert*-butyl groups attached on successive Si atoms cannot be relieved by rotation of the methyl groups about their own axis or by slight distortion of the chain geometry, unless the backbone bonds undergo rotational transitions to states which may be identified with the ridges of high probability in Figure 2d.

Next, we turn our attention to the high-probability ridges and analyze the spatial distribution of atoms of the PDtBS fragment when it assumes a favorable configuration. For a clearer visualization of the interactions between nearest-neighbor side groups, which is mostly responsible for the observed behavior, we confine our attention to two adjacent repeat units. The fragment considered is now a methoxy-terminated molecule of two *tert*-butylsiloxane units. The torsional angles of the central pair of bonds are selected to be on a high-probability ridge, and the molecule is allowed to relax by conventional energy minimization methods.

Two such local minima reached by starting from two configurations in distinct ridges are shown in parts a and b of Figure 7. The central pair of bonds (Si-O, O-Si) assumes the torsional angles (92°, 104°) and (-50°, -30°) in the respective figures. The central bond angle is opened to accommodate the side groups. It measures 169° and 153°, respectively, in parts a and b of Figure 7. Both configurations are found to lead to favorable intramolecular interactions. For the determination of the type of interactions, attractive or repulsive, we consider the

distance between nonbonded atoms and compare their interatomic separation with the van der Waals radii of 2.0, 1.8, 1.6, and 1.2 Å for Si, C, O, and H atoms, respectively. Some of the interatomic separations of interest are indicated in the figures. The shortest separation between H atoms equates to 2.28 Å, which means that attractive interactions occur predominantly between H atoms. As to the interaction between C and H atoms, we may observe a few examples where the separation is smaller than the sum 3.0 Å of the van der Waals radii.

All of the repulsive interactions between C and H atoms occur between the methyl groups belonging to the same *tert*-butyl substituent and will always be present irrespective of the torsional angles of the main chain. The only mechanism to relieve them is the distortion of the bond angles within the *tert*-butyl group itself, and this has no influence on the particular choice of dihedral angles. The interactions between C and H atoms belonging to *tert*-butyl groups on neighboring Si atoms, on the other hand, are essentially attractive and constitute another factor, in addition to the H pairs, favoring the conformations along the high-probability ridges. The corresponding interatomic distances are considerably shorter than those which would occur in the case of methyl substituents instead of *tert*-butyl on Si atoms, which explains the relative preference of the PDtBS fragments for those specific conformations. Finally, we should mention that the side groups come very close to the O and Si atoms and violate the van der Waals radii, but this type of steric interaction is again inherently present in PDtBS and has no relative influence in the particular choice of dihedral angles at the Si-O bonds.

Two conclusions may be drawn from the probability surfaces in Figure 2. First, a description of the bond torsions in terms of three discrete states is far from reflecting the real chain behavior, for $m \geq 2$. A considerably larger number of isomeric states should be adopted, if one chooses to adhere to the RIS formalism in view of its mathematical simplicity. Second, the most stable conformations are necessarily defined by the suitable joint rotations of adjacent bonds centered about the O atom. Thus, it is not possible to define any absolute rotational state preferred by a given backbone bond, but only joint states composed of the specific combinations of pairs of dihedral angles. In this respect, PDAS chains with $m \geq 2$ represent a class of chains where the strong correlations between neighboring bonds i and $i + 1$, flanking the O atom, are of major importance in dictating the conformational statistics and dynamics.

On the basis of those considerations, it seems mathematically convenient to divide the rotational space accessible to a pair of consecutive bonds into 9×9 regions, as schematically depicted in parts a and b of Figure 5, represented each by a pair of dihedral angles (ϕ_i, ϕ_{i+1}), ranking from (-160°, -160°) to (160°, 160°). Dihedral angle pairs which correspond to well-defined ridges and valleys of the probability surfaces are expected to possess statistical weights of comparable magnitude, in conformity with the characteristics of the figures. A quantitative analysis of the equilibrium probabilities of the 81 combinations will be presented next. The objective is to deduce, from probability surfaces, statistical weight parameters which will subsequently be used to estimate unperturbed chain dimensions.

III. Equilibrium Statistics of PDAS

a. Conformation Partition Function. Statistical weights associated with different pairs of dihedral angles

are obtained upon the integration of the probability surfaces over the corresponding regions of the conformational space. In parallel with recent work,³ two steps are involved in this procedure. As a first step, the fractional residence time of any internal backbone bond i in each of the isomeric rotation ranges $\Phi_\alpha \pm 20^\circ$ ($\alpha = 1-9$) is considered, irrespective of the rotational state of the neighboring bonds. Probabilities are assigned to each isomeric range by (i) direct counting of the number of occurrences of all torsional angles (with 2° increments) within those ranges, at intervals of 100 fs, throughout the whole duration of the simulation, (ii) normalization of the dihedral angle distribution curves, and (iii) integration of the normalized probability distribution function over each isomeric range. The probability distribution curve obtained for PDES is shown in Figure 8, as an example. The numbers in the figure represent the probabilities $p_{\alpha,i}$ of each isomeric range $\Phi_\alpha \pm 20^\circ$, for bond i .¹⁹ They are readily used to estimate average first-order interaction energies representative of those ranges. For convenience we will assign indices to the rotameric ranges, from 1 to 9, starting from $-160^\circ \pm 20^\circ$ and ending at $160^\circ \pm 20^\circ$. The planar trans (t) form will have index 5, accordingly. The energy of the trans form will be chosen as a reference state for the first-order interaction energies. Likewise, second-order interaction energies will be expressed relative to that of the tt region.

Let $E_{\alpha,i}$ denote the first-order interaction energy associated with bond i when it assumes the torsional angle $\Phi_\alpha \pm 20^\circ$. $E_{\alpha,i}$ is estimated from

$$E_{\alpha,i} = RT \ln (p_{5,i}/p_{\alpha,i}) \quad (1)$$

where R is the gas constant and T is the absolute temperature. An analogous mathematical treatment applied to slices of the probability surfaces, of thickness 40° , centered about each Φ_α , yields the joint probabilities $p_{\alpha\beta,i}$ of occurrence of the dihedral angles $\Phi_\alpha \pm 20^\circ$ and $\Phi_\beta \pm 20^\circ$ for the respective bonds i and $i-1$. Accordingly, second-order interaction energies $E_{\alpha\beta,i}$ associated with those conformations are evaluated from

$$E_{\alpha\beta,i} = RT \ln (p_{\alpha\beta,i}/p_{\alpha,i}p_{\beta,i}) - E_{\beta,i} + E_{5\alpha,i} \quad (2)$$

Statistical weights $u_{\alpha\beta,i}$ are assigned to the joint states ($\Phi_\alpha \pm 20^\circ$, $\Phi_\beta \pm 20^\circ$) of bonds $i-1$ and i , using the Boltzmann expression

$$u_{\alpha\beta,i} = \exp\{-(E_{\alpha\beta,i} + E_{\beta,i})/RT\} \quad (3)$$

and are organized in 9×9 matrices U_i . Serial multiplication of U_i following conventional methods yields the configuration partition function Z . Inasmuch as two distinct pairs of bonds are present in the siloxane chains, two matrices U_a and U_b , associated with the pair of bonds centered about the Si and O atoms, respectively, are used in the serial multiplication, as

$$Z = U_1[U_a \ U_b]^{x-1}U_n \quad (4)$$

where

$$U_1 \equiv [1 \ 0 \ 0 \ \dots \ 0] \quad (5)$$

and

$$U_n \equiv \text{col} (1 \ 1 \ 1 \ \dots \ 1) \quad (6)$$

The probability that bonds $i-1$ and i occur simultaneously

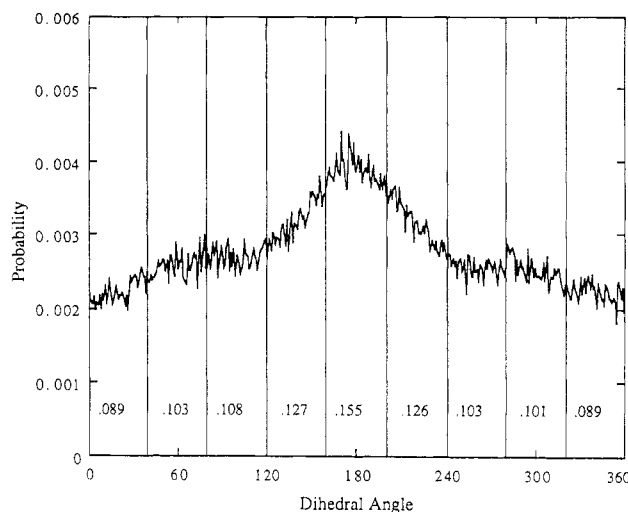


Figure 8. Probability distribution curve for the dihedral angle of the Si-O backbone bond in PDES, irrespective of the state of its neighbors, from MD simulations at 400 K.

in states α and β , respectively, may be recalculated from

$$p_{\alpha\beta,i} = Z^{-1}U_1 \left[\prod_{j=2}^{i-1} U_j \right] U'_{\alpha\beta,i} \left[\prod_{j=i+1}^{x-1} U_j \right] U_n \quad (7)$$

where $2 < i < n$, and $U'_{\alpha\beta,i}$ is the matrix in which all elements other than $u_{\alpha\beta,i}$ are equated to zero. Single-bond dihedral angle probabilities $p_{\alpha,i}$ follow directly from $\sum p_{\beta\alpha,i}$, where the summation is performed over all states accessible to bond $i-1$.

Comparison of the probabilities calculated from eq 7 with those originally resulting from MD simulations verifies the applicability of the statistical weight matrices to treat the equilibrium statistics of the chains. If the deviation between the two sets of probabilities is larger than a limiting value, an iterative scheme starting with the new values, back inserted into eqs 2-5, is undertaken. The criteria adopted in the present work for the establishment of the statistical weights were the following: The standard deviation between two successive iterations k and $k+1$, $\sum_\alpha \sum_\beta [(p_{\alpha\beta,i})_{k+1} - (p_{\alpha\beta,i})_k]^2$, was required to be smaller than that between current probabilities and those corresponding to a freely rotating chain, by at least 1 order of magnitude. These criteria were generally fulfilled without recourse to iterative computation. The resulting probabilities or alternatively the related first- and second-order energies for both types of backbone bond pairs, in all of the PDAS chains presently investigated, are available as supplementary material. Here we report some general trends.

Although chains with larger substituents are highly strained and experience stronger repulsive first-order interactions, the major type of interaction distinguishing the probability distribution of various rotameric states was of second-order origin, i.e., occurring between groups and atoms separated by four or more bonds and dependent on two bond rotation angles. In this respect, the pair of bonds centered about O was of interest, as clearly apparent from the above probability surfaces. The energies were almost constant along a given ridge, showing oscillations of about ± 0.1 kcal/mol in di-*n*-alkyl-substituted siloxanes and ± 0.5 kcal/mol in di-*tert*-butylsiloxanes. Barriers between ridges, as estimated from the equilibrium probabilities of the square regions of conformational space corresponding to the valleys of the probability surfaces, were dependent on the specific type of transition. The passages between ridges A and B in PdtBS

require an activation energy of about 1.5–2.0 kcal/mol, while ridges of the type A were separated by substantially higher (≥ 4.0 kcal/mol) barriers. In parallel with the characteristics of PDtBS, the series of poly(di-*n*-alkylsiloxanes) with $m \geq 2$ exhibit a relatively strong resistance to passage over the $\phi_i = -\phi_{i+1}$ line, while adjacent ridges on either side of the diagonal were separated by barriers of about 1 kcal/mol.

b. Unperturbed Dimensions of PDAS. In the following, we concentrate on a comparative study of the mean-square dimensions of unperturbed PDAS chains, predicted by the present simulations and energy calculations. The mean-square end-to-end distance, $\langle r^2 \rangle_0$, is found from the serial multiplication of generator supermatrices as¹⁰

$$\langle r^2 \rangle_0 = Z^{-1} \mathcal{G}_{[1} [\mathcal{G}_a \ \mathcal{G}_b]^{x-1} \mathcal{G}_n \quad (8)$$

where

$$\mathcal{G}_{[1} = \mathbf{U}_1 \otimes \mathbf{G}_{[1} \quad (9)$$

$$\mathcal{G}_n = \mathbf{U}_n \otimes \mathbf{G}_n \quad (10)$$

$$\mathcal{G}_i = (\mathbf{U}_i \otimes \mathbf{E}_5) \parallel \mathbf{G}_i \parallel, \quad i = a \text{ or } b \quad (11)$$

\mathbf{E}_5 is the identity matrix of order 5, \otimes indicates the direct product, and the matrices $\mathbf{G}_{[1}$ and \mathbf{G}_n are, respectively, the first row and the last column of the 5×5 generator matrix

$$\mathbf{G}_i = \begin{bmatrix} 1 & 2\mathbf{l}^T \mathbf{T} & l^2 \\ 0 & \mathbf{T} & 1 \\ 0 & 0 & 1 \end{bmatrix}_i \quad (12)$$

for bond *i*. \mathbf{G}_i equates to \mathbf{G}_b and \mathbf{G}_a for the two particular cases of $i = [1$ and $i = n]$, respectively. \mathbf{T}_i in eq 12 is the conventional transformation matrix expressing vectorial or tensorial quantities of the bond-based frame $i + 1$, in terms of their representations in frame i .¹⁰ It is a function of the dihedral angle ϕ_i for bond *i* and the supplemental bond angle $\pi - \theta_i$ between bonds *i* and $i + 1$. \mathbf{l}_i is the *i*th bond vector along the chain. Its magnitude is denoted by *l* and equal to 1.64 Å. The superscript T indicates the transpose of a vector. The double bar matrix $\parallel \mathbf{G}_i \parallel$ in eq 11 is the diagonal supermatrix of order 45, whose 9 block elements of order 5 consist of $\mathbf{G}_i(\phi_\alpha)$, with $\phi_\alpha = 1-9$. The subscript *i* is readily replaced by a or b for bonds Si–O, and O–Si, respectively.

The characteristic ratios $C_n = \langle r^2 \rangle_0 / n l^2$ calculated for PDAS at 343 K are shown in parts a and b of Figure 9, for the chains with linear and nonlinear side groups, respectively.²⁰ A gradual increase in C_n is observed with *m* in Figure 9a. An increase in the spherical symmetry of a bulky side group leads to smaller chain dimensions as illustrated in Figure 9b. PDtBS is the polymer with the lowest $C_\infty = \lim_{n \rightarrow \infty} C_n$ value, equal to 5.0, in contrast to PDBS whose C_∞ is equal to 7.6. The limit is evaluated by linear extrapolation of C_n vs $1/n$. The dependence of C_∞ on *m* is shown in Figure 10. A characteristic ratio of 7.7 ± 0.8 is estimated for PDES,²¹ from osmometric and viscosimetric measurements, which compares favorably with the present results. On the other hand, the value of 13 ± 1 reported for the characteristic ratio of PDPS, from viscosimetric measurements on poly(dipropylsiloxane) in two θ solvents,²¹ cannot be rationalized by the present analysis. Such a large increase in unperturbed dimensions of the chain with the increasing length of alkyl group is incom-

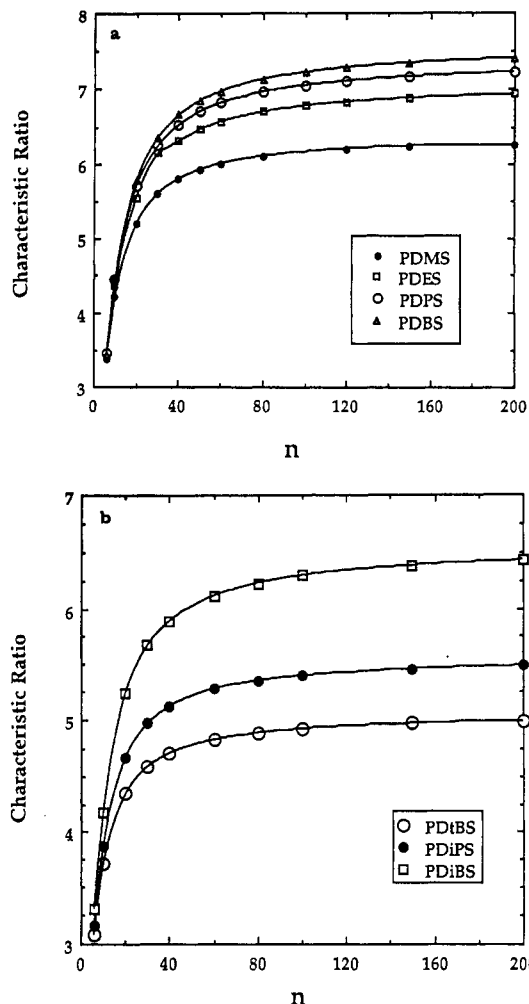


Figure 9. Characteristic ratio C_n of (a) PDMS, PDES, PDPS, and PDBS and (b) PDiPS, PDiBS, and PDtBS, as a function of the number n of backbone bonds, calculated at 343 K.

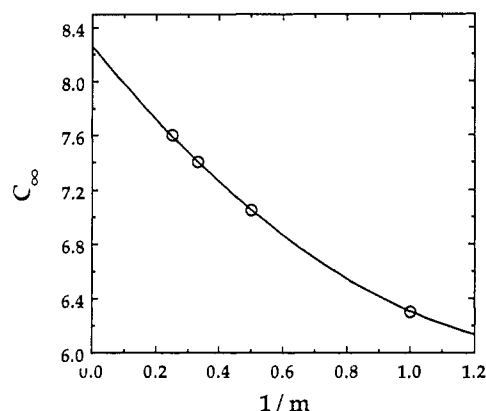


Figure 10. Dependence of C_∞ on the size of the *n*-alkyl substituent, as represented by $1/m$, $m = 1-4$, for PDMS, PDES, PDPS, and PDBS, at 343 K.

patible with theoretical predictions, as was also pointed out in an earlier treatment.²³ Extrapolation provides an estimation of the limiting value of 8.3 for PDAS chains of infinitely long linear side chains.

Previous experimental work indicates that PDMS has a positive temperature coefficient. Recent theoretical analysis with a three-state RIS scheme was not able to reproduce this feature.⁵ The more fine-grained analysis of the conformational space presently carried out yields a negative temperature coefficient, again, unless an opening in bond angles with increasing temperature is taken into

consideration. The superimposition of bond-angle flexibility on rotational isomerization of PDMS is pointed out as a possible explanation for the positive temperature coefficient of PDMS, in a recent work in which 12 rotational isomeric states per bond are considered.²⁴ Exploratory calculations carried out in the present study confirm that changes of $\pm 2^\circ$ in the bond angles θ_a and/or θ_b , over temperature ranges of 100 °C, lead to the required temperature dependence. The unperturbed dimensions are more sensitive to θ_a rather than θ_b . However, MD simulations carried out at two different temperatures, 350 and 450 K, do not indicate a clearly distinguishable increase in the bond angles with a raise in temperature, in order to justify a quantitative approach along this direction.

Acknowledgment. This research was supported by National Science Foundation Grant DMR 89-15025 and Department of Defense University Research Initiative 28747-MS-SM. Partial support from Bogazici University Research Grant 91P0028 is gratefully acknowledged by I.B.

Supplementary Material Available: Tables of first- and second-order interaction energies for seven polymers (5 pages). Ordering information is given on any current masthead page.

References and Notes

- (1) See for example: Mark, J. E. In *Silicon-Based Polymer Science*; Zeigler, J. M., Fearon, F. W. G., Eds.; Advances Chemistry Series 224; American Chemical Society: Washington, DC, 1990; p 47.
- (2) Mark, J. E.; Erman, B. *Rubberlike Elasticity: A Molecular Primer*; Wiley-Interscience: New York, 1988.
- (3) Mattice, W. L.; Dodge, R.; Zuniga, I.; Bahar, I. *Comput. Polym. Sci.* **1991**, *1*, 35.
- (4) Dodge, R.; Mattice, W. L. *Macromolecules* **1991**, *24*, 2709.
- (5) Bahar, I.; Zuniga, I.; Dodge, R.; Mattice, W. L. *Macromolecules* **1991**, *24*, 2986.
- (6) Bahar, I.; Zuniga, I.; Dodge, R.; Mattice, W. L. *Macromolecules* **1991**, *24*, 2993.
- (7) Zuniga, I.; Bahar, I.; Dodge, R.; Mattice, W. L. *J. Chem. Phys.* **1991**, *95*, 5348.
- (8) Cho, D.; Neuburger, N. A.; Mattice, W. L. *Macromolecules* **1992**, *25*, 322.
- (9) Lee, K.-J.; Mattice, W. L. *Comput. Polym. Sci.* **1991**, *1*, 213.
- (10) Flory, P. J. *Statistical Mechanics of Chain Molecules*; Interscience: New York, 1969.
- (11) Bahar, I.; Neuburger, N.; Mattice, W. L. *Macromolecules*, submitted.
- (12) Bahar, I.; Erman, B. *Macromolecules* **1987**, *20*, 1368.
- (13) Tripos Associates, Inc., St. Louis, MO.
- (14) Frierson, M. R. Molecular Mechanics of Group IV Organometallics. Ph.D. Thesis, University of Georgia, Athens, GA, 1984.
- (15) Brooks, B. R.; Bruccoleri, R. E.; Olafson, B. D.; States, D. J.; Swaminathan, S.; Karplus, M. *J. Comput. Chem.* **1983**, *4* (2), 187.
- (16) Polygen Corp., 200 Fifth Avenue, Waltham, MA.
- (17) Grigoras, S.; Lane, T. H. *J. Comput. Chem.* **1988**, *9*, 25. See also: Grigoras, S.; Lane, T. H. In *Silicon-Based Polymer Science*; Zeigler, J. M.; Fearon, F. W. G., Eds.; Advances Chemistry Series 224; American Chemical Society: Washington, DC, 1990; p 7.
- (18) Debolt, L. C.; Mark, J. E. *J. Polym. Sci., Polym. Phys. Ed.* **1988**, *26*, 989.
- (19) Bond serial index i in $p_{\alpha\beta i}$ may be omitted in a given siloxane chain provided that only internal bonds in which end effects are negligibly small are considered. This subscript should be kept in the symbol $p_{\alpha\beta i}$ for joint probabilities of dihedral angles α and β for the respective bonds $i - 1$ and i , inasmuch as two statistically distinct types of bond pairs occur alternately in the backbone.
- (20) Quantitative results obtained for PDMS exactly reproduce those previously obtained⁵ with a three-state scheme. Such a simple approach is not physically justifiable for the higher members of the series, though.
- (21) Mark, J. E.; Chiu, D. S.; Su, T.-K. *Polymer* **1978**, *19*, 407.
- (22) Lee, C. L.; Emerson, F. A. *J. Polym. Sci., Polym. Phys. Ed.* **1967**, *5*, 829.
- (23) Mattice, W. L. *Macromolecules* **1978**, *11*, 517.
- (24) Grigoras, S. *Polym. Prepr. (Am. Chem. Soc., Div. Polym. Chem.)* **1991**, *32* (2), 720.